

# Effects of a Nonligating Pendant Hydrogen-Bonding Group in a Metal Complex: Stabilization of an HF Complex

Dong-Heon Lee, Hye J. Kwon, Ben P. Patel, Louise M. Liable-Sands, Arnold L. Rheingold,\* and Robert H. Crabtree\*

Department of Chemistry, Yale University, P.O. Box 208107, New Haven, Connecticut 06520-8107, and Department of Chemistry, University of Delaware, Newark, Delaware 19716

Received December 3, 1998

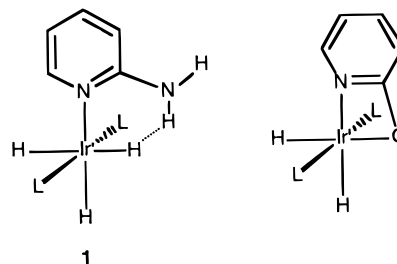
An amino group has been appended to a benzoquinolinato ligand (bq-NH<sub>2</sub> or bq-NH(*i*-Pr)) in such a way that it can hydrogen bond to a ligand that is also bound to the metal. The effects of this two-point binding are studied. The complexes [(bq-NHR)IrH(L)(PPh<sub>3</sub>)<sub>2</sub>]BF<sub>4</sub> (R = H, *i*-Pr) were synthesized where L = H<sub>2</sub>O, F. The hydrogen-bonding pattern in the water complex is probed by crystallographic, IR, and NMR studies. The fluoro complexes protonate at -90 °C to give unstable hydrogen fluoride complexes, characterized by NMR (<sup>1</sup>J<sub>HF</sub> = 440 Hz, bq-NH<sub>2</sub>; 430 Hz, bq-NH(*i*-Pr)). Comparison with results for the corresponding bq-H and bq-CH<sub>3</sub> species suggests that the hydrogen bonding provided by the pendant amino group is the key factor that allows stabilization of the HF complex, a previously unknown species. Crystal structures of an aqua and a fluoro derivative are reported.

## Introduction

We have attached hydrogen-bonding pendant groups to a number of ligands so that the pendant groups are unable to bind directly to the metal, but can hydrogen bond to the adjacent ligand.<sup>1</sup> If properly placed, these groups could have effects similar to those of hydrogen-bonding residues in the active site cavity of metalloenzymes, which are believed to contribute to the acceleration of enzyme reactions by transition-state stabilization.<sup>2</sup>

In prior work,<sup>1</sup> we showed how 2-aminopyridine can form an intramolecular H···H hydrogen bond between the pendant amino group and the adjacent hydride as in complex **1**, but this system is not rigid and the pendant group can bind to the metal under certain conditions. For instance, when 2-hydroxypyridine replaces aminopyridine in **1**, H<sub>2</sub> is lost and the cyclometalated product shown is formed.<sup>3</sup> To avert this possibility, we have now induced rigidity in the system by using rigid cyclometalated benzoquinoline ligands in which amino-substitution is easy. We report here the effect of the pendant group on the stabilization of an HF complex (M–F–H).

As mentioned in a review by Richmond,<sup>4</sup> a number of groups have described N–H···F species.<sup>4</sup> Bifluoride<sup>5</sup> complexes, containing the group M–F···H–F, can be considered as examples of intermolecular hydrogen



bonding involving a metal fluoride complex and outer sphere HF. A relevant communication has appeared on some of our work.<sup>6</sup> An article giving X-ray structural evidence suggesting that discrete HF ligands are coordinated to a lanthanide in a complex inorganic salt has appeared more recently.<sup>7</sup>

**Choice of System.** 7,8-Benzoquinoline<sup>8</sup> and its derivatives<sup>6</sup> readily cyclometalate with [Ir(cod)(PPh<sub>3</sub>)<sub>2</sub>]BF<sub>4</sub> under H<sub>2</sub> to give a benzoquinolinato complex, **2** (eq 1). We have extensive reactivity data<sup>8</sup> on both **2** and its derivatives. The labile coordination site on the metal in **2**, trans to the high trans effect aryl ligand, is the reactive site for the chemistry of the complex. The 2-position of free benzoquinoline is easy to substitute selectively with NaNH<sub>2</sub> or LiNH(*i*-Pr) via the Chichibabin reaction.<sup>9</sup> These amino groups were chosen because they are versatile and can in principle act as hydrogen bond donors via NH, or as acceptors or bases via the lone electron pair. The amino-substituted ben-

(1) (a) Peris, E.; Lee, J. C., Jr.; Crabtree, R. H. *J. Chem. Soc., Chem. Commun.* **1994**, 2573. (b) Peris, E.; Lee, J. C., Jr.; Rambo, J. R.; Eisenstein, O.; Crabtree, R. H. *J. Am. Chem. Soc.* **1995**, *117*, 3485.

(2) Walsh, C. *Enzymatic Reaction Mechanisms*; Freeman: San Francisco, 1979.

(3) Lee, J. L.; Crabtree, R. H. Unpublished data.

(4) Richmond, T. G. *Coord. Chem. Rev.* **1990**, *105*, 221.

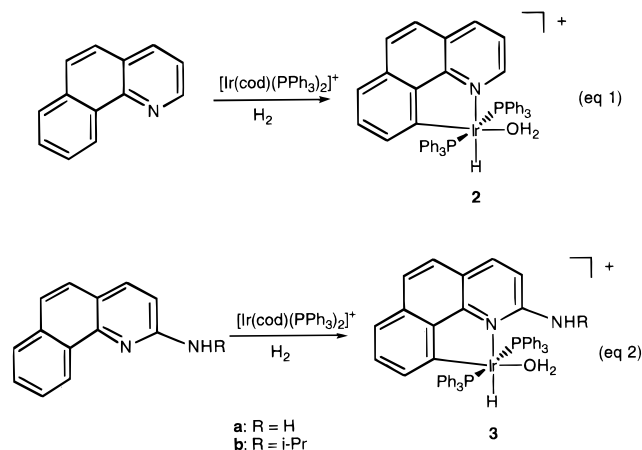
(5) (a) Murphy, V. J.; Hascall, T.; Chen, J. Y.; Parkin, G. *J. Am. Chem. Soc.* **1996**, *118*, 7248. (b) Whittesley, M. K.; Perutz, R. N.; Greener, B.; Moore, M. H. *J. Chem. Soc., Chem. Commun.* **1997**, 187. (c) Hintermann, S.; Pregosin, P. S.; Rügger, H. *J. Organomet. Chem.* **1992**, *435*, 225.

(6) Patel, B. P.; Crabtree, R. H. *J. Am. Chem. Soc.* **1996**, *118*, 13105. (7) Mazej, Z.; Borrmann, K. L.; Zemva, B. *Inorg. Chem.* **1998**, *37*, 5912.

(8) (a) Crabtree, R. H.; Lavin, M.; Bonneviot, L. *J. Am. Chem. Soc.* **1986**, *108*, 4032. (b) Lavin, M.; Holt, E. M.; Crabtree, R. H. *Organometallics* **1989**, *8*, 99.

(9) (a) Vorbrüggen, H. *Adv. Heterocycl. Chem.* **1990**, *49*, 117. (b) Khristich, B. I.; Kruchinin, V. A.; Pozharskii, A. F.; Siminov, A. M. *Chem. Heterocycl. Compounds* **1971**, 759.

zoquinoline ligands also readily cyclometalate, and in the resulting complexes, **3** (eq 2) (R = NH<sub>2</sub>, **a**; NH(*i*-Pr), **b**), the pendant groups are necessarily adjacent to the labile site, allowing interaction between the pendant groups and a ligand bound to Ir. At the same time, the rigidity of the system prohibits ligation of the amino group to the metal, which would block reactivity and complicate the analysis.



## Results

**Synthesis of the Ligand and Starting Complexes.** The known 2-amino-7,8-benzoquinoline ligand (bq-NH<sub>2</sub>)<sup>10</sup> and new 2-isopropylamino-7,8-benzoquinoline (bq-NH(*i*-Pr)) ligand were readily synthesized (yield 88%, bq-NH<sub>2</sub>; 70%, bq-NH(*i*-Pr)) by a Chichibabin reaction<sup>9</sup> between NaNH<sub>2</sub> or LiNH(*i*-Pr) and 7,8-benzoquinoline in a xylenes/*N,N*-dimethylaniline mixture at 177 °C. Characterization data support the formulation: the microanalysis, the strong parent ion peak at 194 and 236 amu in the GC/MS spectrum, and the strong NH stretching vibrations at 3411 and 3415 cm<sup>-1</sup> in the thin-film IR spectrum are consistent with the formulation of bq-NH<sub>2</sub> and bq-NH(*i*-Pr), respectively. The crystal structures of the iridium complexes, discussed below, indicate that the amino groups are indeed at the 2-position, consistent with the expected outcome of the Chichibabin reaction.

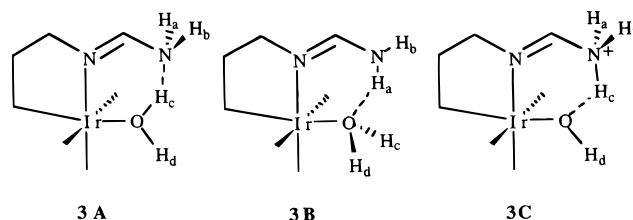
The aminated ligands react smoothly with [Ir(cod)(PPh<sub>3</sub>)<sub>2</sub>]BF<sub>4</sub> (cod = 1,5-cyclooctadiene) in wet CH<sub>2</sub>Cl<sub>2</sub> under H<sub>2</sub> (1 atm) at 0 °C to give the cyclometalated species, [(bq-NHR)IrH(H<sub>2</sub>O)(PPh<sub>3</sub>)<sub>2</sub>]BF<sub>4</sub>, **3** (R = H, **a**; *i*-Pr, **b**), with pendant amino groups in 70% (**3a**) or 78% (**3b**) yield; this is the same route<sup>8b</sup> that was previously used for **2**. The close analogy between the <sup>1</sup>H NMR spectra of **3a** and those of the crystallographically characterized species **2**<sup>8</sup> and **3b** (see below) confirms the proposed structure. In particular, the Ir–H (**2**, –16.1 ppm {t, *J*<sub>HP</sub> = 14 Hz}; **3a**, –16.4 ppm {t, *J*<sub>HP</sub> = 14.6 Hz}; **3b**, –16.1 ppm {t, *J*<sub>HP</sub> = 14.4 Hz}) and Ir–OH<sub>2</sub> (**2**, 2.54 ppm {s}; **3a**, 3.06 ppm {s} at –50 °C; **3b**, 2.78 {s} at –40 °C) proton resonances (s = singlet, t = triplet) appear very similar. The hydride chemical shift is consistent<sup>11</sup> with a stereochemistry having the hydride

trans to N, not to C or P. In addition, compound **3a** shows an Ar–NH<sub>2</sub> resonance at 6.09 ppm (broad), and **3b** shows an Ar–NH resonance at 6.16 ppm (d, *J*<sub>HP</sub> = 6.6 Hz at –10 °C). The <sup>31</sup>P NMR spectra show one peak (**3a**, 20.3 ppm; **3b**, 20.42 ppm), at a position consistent with the proposed structures.

### Hydrogen Bonding in the Aqua Complexes (**3**).

The hydrogen-bonding pattern in **3** was a point of particular interest. Of the three most likely structures, **3A**, **3B**, and **3C**, evidence from variable-temperature <sup>1</sup>H NMR (CD<sub>2</sub>Cl<sub>2</sub>) and IR spectroscopic studies of **3a** and **3b** enabled us to choose a plausible model.

Results of the NMR studies of **3a** and **3b** rule out structures **A** and **C** as possible hydrogen-bonding models. The two structures require that the two protons of the bonded water are inequivalent and would thus yield two peaks when hydrogen-bonded. In the two complexes, however, the bound water resonance starts appearing at 233 K as broad single peaks (**3a**, 3.06 ppm; **3b**, 2.78 ppm) and sharpens and shifts (**3a**, 2.90 ppm; **3b**, 2.81 ppm) as the temperature is lowered to 193 K. Structure **B** is also apparently inconsistent with the data, which predict two peaks for the two hydrogens of the pendant amino group, but from the singlet –NH<sub>2</sub> resonance observed in **3a** (6.09 ppm, 293 K; 6.24 ppm, 193 K) we assume that the two hydrogens (a and b) of the amino group exchange rapidly by C–N bond rotation in solution even at low temperatures. The thin-film IR spectroscopic study shows two distinctive ν(NH) stretching bands at 3478 and 3365 cm<sup>-1</sup>, both shifted from the single band (3411 cm<sup>-1</sup>) that we observe in the free ligand, suggesting that **3B** is the likely hydrogen-bonding mode, at least in the solid state. From the resonances of the –NH– peak of the **3b** pendant group (6.24 ppm (br s), 293 K; 6.24 ppm (d, *J*(H–N–C–H) = 8.6 Hz), 263 K; 6.51 ppm (d), 213 K) and one ν(NH) band observed at 3377 cm<sup>-1</sup> (shifted to a lower energy from 3415 cm<sup>-1</sup> of the free ligand) we conclude by analogy that the lone hydrogen of the –NH(*i*-Pr) group also hydrogen bonds with the lone electron pair of the water oxygen in a similar way to structure **3B**.



**Crystal Structure of **3b**.** To examine the hydrogen-bonding pattern in the complexes, we obtained a crystal structure of **3b** as the triflate salt, the only salt that would crystallize well. The resulting structure (Figure 1, Tables 1 and 2) shows that the benzoquinoline ligand is indeed 2-substituted as expected and that the triflate anion is located in the vicinity of the cation.

Hydrogen bonding between the hydrogen of –NH(*i*-Pr) and lone pair of bound water oxygen is also confirmed: the O⋯H–N distance and angle in the crystal are calculated as 2.302 Å and 155.6° (on the basis of a planar sp<sup>2</sup> N with *d*(N–H) = 1.03 Å), consistent with a hydrogen-bonding model of type **3B**.

**Synthesis of the Fluoride.** To better test the idea that the pendant –NH<sub>2</sub> group can hydrogen bond to a

(10) Bergstrom, F. W. *J. Org. Chem.* **1938**, *3*, 424.

(11) (a) Crabtree, R. H.; Demou, P. C.; Eden, D.; Mihelcic, J. M.; Parnell, C. A.; Quirk, J. M.; Morris, G. E. *J. Am. Chem. Soc.* **1992**, *114*, 6994. (b) Crabtree, R. H.; Faller, J. W.; Mellea, M. F. *Organometallics* **1982**, *1*, 1361.

Table 1. Crystal Data and Structure Refinement for  $3b \cdot CF_3SO_3 \cdot CH_2Cl_2$  and **4a**

	$3b \cdot CF_3SO_3 \cdot CH_2Cl_2$	<b>4a</b>
empirical formula	$C_{54}H_{50}Cl_2F_3IrN_2O_4P_2S$	$C_{49}H_{40}FIrN_2P_2$
fw	1205.06	929.97
temp (K)	173(2)	173(2)
wavelength (Å)	0.71073	0.71073
cryst syst	triclinic	monoclinic
space group	$P\bar{1}$	$P2_1/c$
unit cell dimensions		
<i>a</i> (Å)	10.6226(2)	16.0434(4)
<i>b</i> (Å)	11.7354(2)	13.8092(4)
<i>c</i> (Å)	20.6503(3)	18.9100(5)
α (deg)	82.3766(7)	90
β (deg)	87.7899(2)	114.327(1)
γ (deg)	82.5466(10)	90
volume (Å <sup>3</sup> ), <i>Z</i>	2529.38(5), 2	3817.46(18), 4
density (calcd) (g/cm <sup>3</sup> )	1.582	1.618
abs coeff (mm <sup>-1</sup> )	2.909	3.625
<i>F</i> (000)	1208	1856
cryst dimens (mm)	0.30 × 0.15 × 0.01	0.30 × 0.20 × 0.20
θ range for data collection (deg)	1.76–26.00	1.89–23.00
limiting indices	−13 ≤ <i>h</i> ≤ 13, −14 ≤ <i>k</i> ≤ 14, 0 ≤ <i>l</i> ≤ 25	−17 ≤ <i>h</i> ≤ 16, −15 ≤ <i>k</i> ≤ 13, −20 ≤ <i>l</i> ≤ 20
no. of reflns collected	16608	9547
no. of ind reflns	9321 ( $R_{int} = 0.1199$ )	4667 ( $R_{int} = 0.1160$ )
transmission factors	1.000 and 0.590	0.5309 and 0.4093
refinement method	full-matrix least-squares on $F^2$	full-matrix least-squares on $F^2$
no. of data/restraints/param	9321/0/622	4667/0/481
goodness-of-fit on $F^2$	0.854	1.101
final <i>R</i> indices [ $I > 2\sigma(I)$ ]	$R_1 = 0.0609$ , $wR_2 = 0.1314$	$R_1 = 0.0382$ , $wR_2 = 0.1029$
<i>R</i> indices (all data)	$R_1 = 0.1145$ , $wR_2 = 0.1615$	$R_1 = 0.0153$ , $wR_2 = 0.1185$
largest diff peak and hole (e Å <sup>-3</sup> )	2.259 and −2.828	1.108 and −0.791

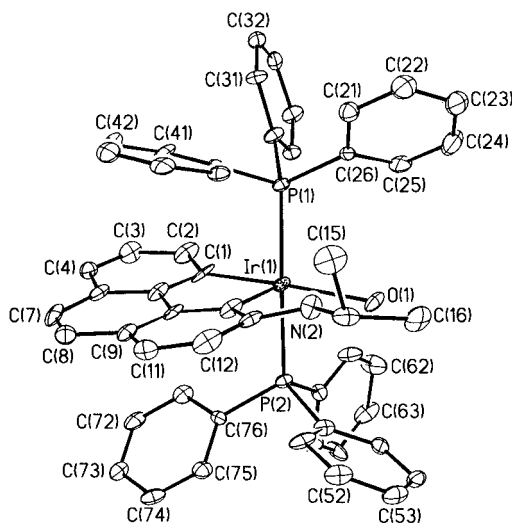


**Figure 1.** ORTEP diagram of  $[(bq-NH(i-Pr))Ir(H)(H_2O)(PPh_3)_2](CF_3SO_3) \cdot CH_2Cl_2$  (**3b**· $CF_3SO_3 \cdot CH_2Cl_2$ ). Thermal ellipsoids shown at 30% probability. Hydrogen atoms, counterion, and solvent molecule are omitted for clarity.

ligand bound to Ir, we synthesized analogous fluoro-complexes, with the hope that  $J(H,F)$  coupling between the amino and fluoro groups would unequivocally identify any hydrogen bonding. The aqua complexes proved to react rapidly with  $[n-Bu_4N]F$  (TBAF) in acetone at room temperature to give analogous fluoride complexes,  $(bq-NHR)IrH(F)(PPh_3)_2$ , **4** (eq 3) ( $R = H$ , **a**;  $i-Pr$ , **b**). In addition,  $(bq-CH_3)IrH(F)(PPh_3)_2$  (**4c**) was synthesized as a control:  $bq-CH_3$ <sup>12</sup> has the same steric effects as the aminated ligands but cannot hydrogen bond and is thus an ideal control ligand. **4a** was obtained in 65% yield after recrystallization from  $CH_2Cl_2$ /hexanes, and **4b** was

**Table 2.** Selected Bond Lengths and Angles for Complexes  $3b \cdot CF_3SO_3 \cdot CH_2Cl_2$  and **4a**

	Bond Distances (Å)			
	<b>3b</b>		<b>4a</b>	
Ir(1)–P(1)	2.309(3)	Ir(1)–C(11)	2.009(8)	
Ir(1)–P(2)	2.349(3)	Ir(1)–F(1)	2.143(4)	
Ir(1)–O(1)	2.276(6)	Ir(1)–N(1)	2.168(6)	
Ir(1)–N(1)	2.190(8)	Ir(1)–P(1)	2.3047(19)	
Ir(1)–C(1)	2.005(10)	Ir(1)–P(2)	2.3165(19)	
N(1)–C(13)	1.361(12)	N(1)–C(1)	1.331(10)	
N(2)–C(13)	1.342(14)	N(2)–C(1)	1.343(10)	
N(2)–C(14)	1.469(12)			
C(14)–C(15)	1.510(16)			
C(14)–C(16)	1.516(17)			
	Bond Angles (deg)			
	<b>3b</b>		<b>4a</b>	
C(1)–Ir(1)–N(1)	80.3(4)	C(11)–Ir(1)–N(1)	80.3(3)	
C(1)–Ir(1)–O(1)	177.3(4)	C(11)–Ir(1)–F(1)	174.8(2)	
C(1)–Ir(1)–P(1)	87.6(3)	C(11)–Ir(1)–P(1)	86.7(2)	
C(1)–Ir(1)–P(2)	92.3(3)	C(11)–Ir(1)–P(2)	86.2(2)	
N(1)–Ir(1)–O(1)	98.5(3)	N(1)–Ir(1)–F(1)	95.54(19)	
N(1)–Ir(1)–P(1)	92.0(2)	N(1)–Ir(1)–P(1)	92.85(16)	
N(1)–Ir(1)–P(2)	90.8(2)	N(1)–Ir(1)–P(2)	92.39(16)	
O(1)–Ir(1)–P(1)	94.8(2)	F(1)–Ir(1)–P(1)	90.29(12)	
O(1)–Ir(1)–P(2)	85.4(2)	F(1)–Ir(1)–P(2)	97.18(12)	
P(1)–Ir(1)–P(2)	177.17(11)	P(1)–Ir(1)–P(2)	170.42(7)	
N(1)–C(13)–N(2)	116.5(10)	N(1)–C(1)–N(2)	117.7(7)	
C(13)–N(2)–C(14)	125.1(10)			
N(2)–C(14)–C(15)	110.7(9)			
N(2)–C(14)–C(16)	108.3(10)			

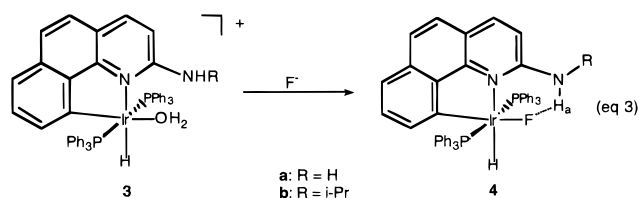
obtained in 70% yield after recrystallization. **4c** was obtained in 73% yield.

Apart from the microanalysis, crystallographic (see below) and spectroscopic evidence support the structure of **4a**, **4b**, and **4c**. In particular, the Ir–H resonances at −16.13 ppm (**4a**), −16.09 ppm (**4b**), and −17.5 ppm (**4c**) show coupling not only to the *cis* PPh<sub>3</sub> groups (<sup>2</sup> $J(H,P)$  {*t*} 17 Hz, **a**; {*t*} 16.7 Hz, **b**, {*t*} 15 Hz, **c**) but also to the *cis* fluoride (<sup>2</sup> $J(H,F)$  {*d*} 4.8 Hz, **a**; {*d*} 5.6

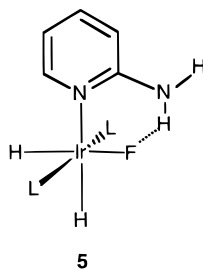
(12) Arai, S.; Ishikura, M.; Sato, K.; Yamagishi, T. *J. Heterocycl. Chem.* **1995**, *32*, 1081.



Hz, **b**, {d} 4.7 Hz, **c**). The  $^{19}\text{F}$  NMR of **4a** shows a resonance at  $-328$  ppm (vs  $\text{CFCl}_3$ ) with a triplet coupling to the cis  $\text{PPh}_3$  groups ( $^2J(\text{F},\text{P})$  {t} 21 Hz).



The key observation supporting a hydrogen-bonding interaction is the presence at 193 K of a  $J(\text{H}_a,\text{F})$  coupling of 52 Hz in one of the amino resonances at 10.1 ppm in the fluoride **4a**, assigned to  $\text{H}_a$ . Similar  $J(\text{H},\text{F})$  coupling of 49.6 Hz for the lone proton of  $-\text{NH}(\textit{i}\text{-Pr})$  is also shown at 193 K. These numbers are appropriate for a hydrogen-bonding interaction of the type  $\text{N}-\text{H}_a\cdots\text{F}$  by comparison with the value of 63.5 Hz previously observed<sup>1a</sup> for the appropriate rotamer of the related 2-aminopyridine fluoride **5**. This is confirmed in **4a** by the presence of  $\nu(\text{NH})$  bands in the IR spectrum at 3470 and 3354  $\text{cm}^{-1}$ , shifted relative to the 3411  $\text{cm}^{-1}$  band in the free ligand, and comparable to that previously found in fluoride **5**. In **4b**, the  $\nu(\text{NH})$  band is too broad (3300–3450  $\text{cm}^{-1}$ ) for a precise wavenumber to be reported.



A variable-temperature proton NMR study of the fluoride **4a** gave further information. On cooling, the  $-\text{NH}_2$  resonance decoalesces, and by 193 K,  $\text{H}_a$  and  $\text{H}_b$  appear as broad singlets at 4.8 and 10.1 ppm. Averaging these shifts, we infer that the coalesced signal must occur near 7.45 ppm, hidden under the large aromatic signal at room temperature. Line shape analysis between 183 and 193 K reveals a significant initial broadening that was interpreted in terms of an exchange rate at 193 K. The free energy barrier,  $\Delta G^\ddagger_{193\text{K}}$ , for  $\text{H}_a/\text{H}_b$  exchange was then estimated by standard methods as 12.4 ( $\pm 0.5$ ) kcal/mol.<sup>1a</sup> As we have discussed previously,<sup>13</sup> this barrier is expected to include the intrinsic  $\text{Ar}-\text{NH}_2$  rotation barrier, previously estimated as 5.7 kcal/mol, and the contribution from the hydrogen bond strength, which is therefore estimated as 6.7 ( $\pm 1$ ) kcal/mol. This  $\text{N}-\text{H}\cdots\text{F}$  hydrogen bond strength is comparable to the value of 5.2 ( $\pm 1$ ) kcal/mol previously estimated for the aminopyridine analogue, **5**.

**Crystallographic Study of 4a.** Complex **4a** gave crystals suitable for a complete X-ray diffraction study, shown in Figure 2 and Tables 1 and 2.

This shows that the structure of the complex is consistent with the postulated structure: the fluoride is located trans to the aryl ligand and hydrogen bonds

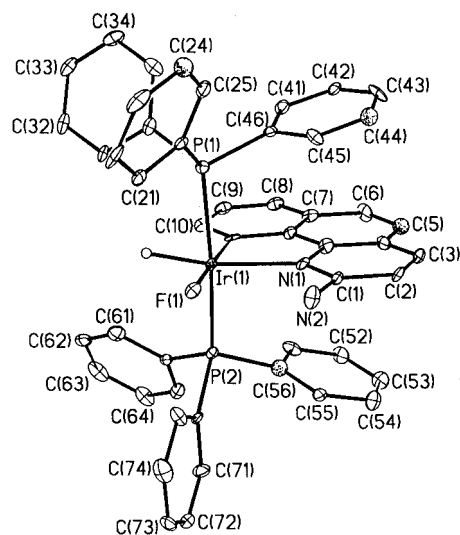


**Figure 2.** ORTEP diagram of  $[(\text{bq}-\text{NH}_2)\text{Ir}(\text{H})(\text{F})(\text{PPh}_3)_2]$  (**4a**). Thermal ellipsoids shown at 30% probability. Hydrogen atoms, except for hydride, are omitted for clarity. Carbon atoms that were refined isotropically are shown as spheres.

to one of the hydrogens of the  $\text{NH}_2$  pendant group. The  $\text{H}\cdots\text{F}$  distance and  $\text{N}-\text{H}\cdots\text{F}$  angle found in the crystal are 1.813 Å and 165.6°, respectively, consistent with the classical hydrogen-bonding model.

**Spectroscopic Detection of a Hydrogen Fluoride Complex.** In their classic 1958 text, Basolo and Pearson<sup>14</sup> indicate that the acid catalysis of fluoride substitution in  $\text{Co}(\text{III})$  complexes implies that the fluoride ligand can be protonated to give a transient hydrogen fluoride complex of the type  $\text{M}-\text{F}-\text{H}$ , which rapidly loses HF. Only one proposed HF complex<sup>7</sup> has so far been isolated, however, and the alternative hydrogen-bonded adduct,  $\text{M}-\text{F}\cdots\text{H}-\text{A}$  ( $\text{HA} = \text{acid}$ ), cannot be excluded on kinetic evidence alone.

Protonation of the pendant amine fluoro-complex, **4a**, with  $\text{HBF}_4\cdot\text{Et}_2\text{O}$  at 195 K in  $\text{CD}_2\text{Cl}_2$  leads to the formation of the protonated form, **6a**, in solution (eq 4). The complex decomposed on attempted isolation, but the  $^1\text{H}$  NMR data at 183 K of **6a** indicated it is a hydrogen fluoride complex. In particular, the resonances at 10.1 and 4.8 ppm, assigned to the  $-\text{NH}_2$  group, are replaced by new ones at 9.8 and 6.8 ppm in a 1:2 integral ratio and assigned to  $\text{H}_a$  and ( $\text{H}_b + \text{H}_c$ ) (see eq 4), respectively. This assignment is supported by the observation of rapid ( $\ll 1$  min) isotope exchange of  $\text{H}_a$ ,  $\text{H}_b$ , and  $\text{H}_c$  with  $\text{CD}_3\text{-OD}$  ( $^1\text{H}$  NMR). The key observation is the presence of a  $^1J(\text{H},\text{F})$  coupling of 440 Hz for the  $\text{H}_a$  resonance, consistent with **6a** being a true  $\text{N}\cdots\text{H}-\text{F}$  complex, rather than having a hydrogen-bonded  $\text{N}-\text{H}\cdots\text{F}$  system, as in **4a**, where  $^1J(\text{H},\text{F})$  is much lower (e.g., 52 Hz for **4a**). Figure 3 illustrates the  $\text{H}_a$  resonances of **4a** and **6a**.

A similar effect is observed upon protonation of the related complex **4b** at 183 K, where  $^1J(\text{H},\text{F})$  is 430 Hz.

As expected, the  $^1J(\text{H},\text{F})$  coupling was the same at 300 and at 500 MHz. The 440 Hz coupling involves  $\text{H}_a$  and F because the same 440 Hz coupling appears in the  $^{19}\text{F}$  NMR spectrum but disappears on decoupling the

(13) Sandstrom, J. *Dynamic NMR Spectroscopy*; Academic Press: New York, 1982.

(14) Basolo, F.; Pearson R. G. *Mechanisms of Inorganic Reactions*; Wiley: New York, 1958; p 153.

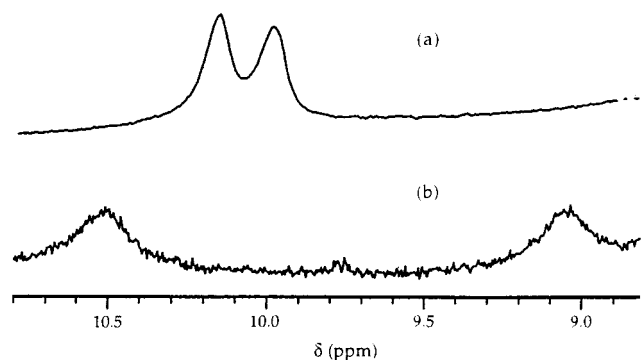
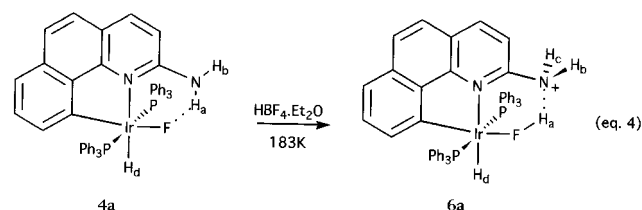


**Figure 3.** N–H–F–Ir and N··H–F–Ir proton resonances in the 300 MHz  $^1\text{H}$  NMR spectra of **4a** (a) and **6a** (b) at 183 K.



$\text{H}_a$  resonance of **6**. The protonation of the bq- $\text{CH}_3$  species **4c** did not lead to a stable H–F complex, indicating that the N··H–F stabilization is not the result of a steric effect, but of the hydrogen-bonding ability of the  $\text{NH}_2$  pendant ligand.

The large value of  $^1J(\text{H}_a, \text{F})$ , 440 Hz, observed for **6a** is reasonable for an H–F complex, as indicated by comparison with literature data.<sup>15</sup> Figure 4 illustrates the relation between  $J$  and  $\delta$  values for HF in the gas phase, in various hydrogen-bonded adducts, such as  $[\text{C}_5\text{H}_5\text{N}\cdots\text{H}-\text{F}]$ , in solution, and in  $[\text{FHF}]^-$  ion, also in solution.

The hydrogen-bonded adducts of nitrogen bases with HF and the HF complex **6** are clustered in the same region of the graph, while HF (gas phase) and  $[\text{FHF}]^-$  ion have quite different spectral properties. This is powerful supporting evidence that the  $\text{H}_a$  resonance indeed arises from a hydrogen-bonded HF group. The recently discovered bifluoride complexes also have distinctly different NMR spectral behavior.<sup>5a</sup>

We needed to establish if the fluoride remains bound to the metal on protonation. The Ir–F bond in **4a** is indeed retained in **6a**, as shown by the persistence of a cis-coupling between the phosphorus nuclei of L and the cis fluoride in the  $^1\text{H}$  NMR spectrum on going from **4a** ( $J(\text{P}, \text{F}) = 21$  Hz) to **6a** ( $J(\text{P}, \text{F}) = 12$  Hz). In further support of this structure, a doublet resonance at 16.8 ppm with a  $^2J(\text{P}, \text{F})$  coupling of 21 Hz in the  $^{31}\text{P}\{^1\text{H}\}$  NMR spectrum of **4a** moves in **6a** to 21.5 ppm but retains some coupling, 12 Hz. Protonation of the fluoride is expected to weaken the Ir–F bond, and so the observed decrease in the coupling is reasonable.

The metal-bound H–F in **6a** is certainly hydrogen-bonded, as indicated by the data<sup>15</sup> of Figure 4, and the pendant amino group of the ligand seems the most natural H-bond acceptor group to consider. Consistent with this proposal, irradiation of the  $\text{H}_a$  proton causes a slight narrowing of the broad  $\text{H}_{c,d}$  amine resonance, probably as a result of unresolved coupling between  $\text{H}_a$  and  $\text{H}_{c,d}$ .

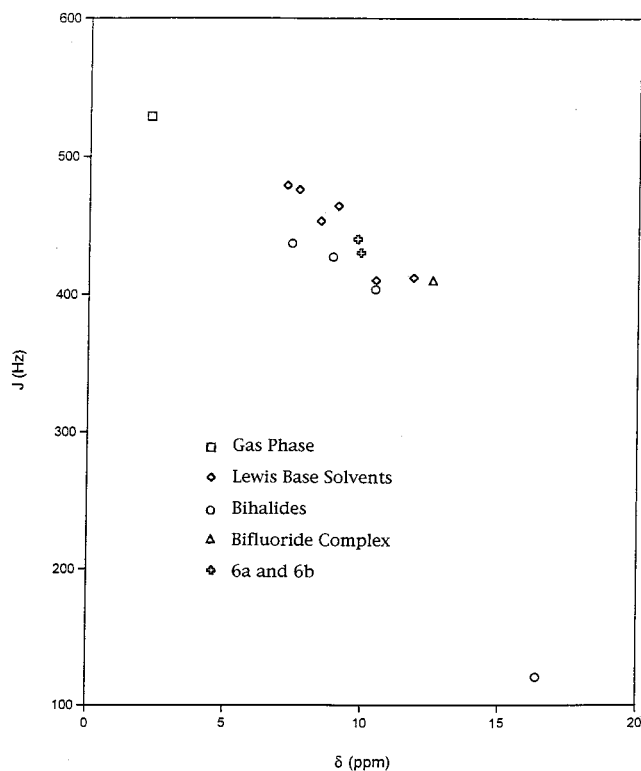


**Figure 4.**  $^1J_{\text{HF}}$  vs  $\delta$  correlation plot of data from ref 17 (bifluoride complex from ref 5a), showing close agreement with the data points for **6a** and **6b**.

The kinetic site of protonation<sup>16</sup> of **4a** to give **6a** could not be determined experimentally, but protonation of the basic amino nitrogen seems most likely. This is expected to be followed by proton transfer from the resulting  $\text{NH}_3^+$  group to the hydrogen-bonded fluoride to give **6a**. The  $\text{p}K_a$  of HF (ca. 4 in water) is at the high end of the reported  $\text{p}K_a$  range for  $\text{ArNH}_3^+$  (–10 to 5), consistent with the postulated direction of the proton transfer to give **6a**.<sup>17</sup>

The stability of the HF complex is indeed a result of the presence of the pendant hydrogen-bonding amino group: as already stated, by substituting bq- $\text{CH}_3$  for bq- $\text{NH}_2$ , the fluoro complex no longer gives an HF complex on protonation under identical conditions and merely loses HF. Free HF is not observed in solution, but control experiments with deliberate addition of HF show that this is because free HF does not survive under the conditions used; recent data from Caulton<sup>18</sup> indicate that free HF can rapidly react with the glass of an NMR tube to give  $[\text{SiF}_5]^-$ .

## Discussion

The data indicate that the presence of a pendant  $-\text{NH}_2$  or  $-\text{NH}_3^+$  group can have significant “neighboring group” effects on the reactivity of ligands bound to a metal at an adjacent site. In the case of the fluoro complex, **4a**, the pendant  $-\text{NH}_2$  group allows stabilization of a very labile HF complex to a sufficient degree that it can be spectroscopically detected.

(16) Kramarz, K. W.; Norton, J. R. *Prog. Inorg. Chem.* **1990**, *42*, 1.

(17) Bordwell, F. G. *Acc. Chem. Res.* **1988**, *21*, 456.

(18) Cooper, A. C.; Huffman, J. C.; Caulton, K. G. *Inorg. Chim. Acta* **1998**, *270*, 261.

(15) Martin, J. S.; Fujiwara, F. Y. *J. Am. Chem. Soc.* **1974**, *96*, 7632.

The observation of an HF complex helps confirm the proposal that acid-catalysis of fluoride substitution occurs by prior protonation at the fluoride and loss of the labile HF ligand. We and others have previously provided evidence for halocarbon complexes where the order of binding is  $RF < RCl < RBr < RI$ .<sup>19</sup> Here we see that, at least in the special case of HF, a weak acid, a similar type of complex can also exist.

### Conclusion

The presence of a potentially hydrogen-bonding but nonligating group at the 2-position of a cyclometalated benzoquinolinato iridium complex has significant effects on the chemistry of ligands adjacent to the group, as compared to a control compound with a pendant group showing similar steric effects without the hydrogen-bonding ability. Here we show that the group hydrogen bonds to an adjacent Ir–F fluoride and stabilizes an Ir–(FH) complex. In other work,<sup>20</sup> we find it also acts as a base in facilitating the activation of molecular hydrogen and modifies the structure of a trihydride derived from protonating the neutral dihydride starting complex (**1**). For example, in the absence of the amino group, a stable H<sub>2</sub> complex is formed by displacement of H<sub>2</sub>O; with the amino group present, proton transfer from this H<sub>2</sub> complex to the bq-NH<sub>2</sub> group occurs.<sup>20</sup> This general strategy may in the future offer other unusual applications for modifying ligand structure and reactivity in metal complexes.

### Experimental Section

All reactions were carried out with standard Schlenk techniques and degassed analytical grade solvents under N<sub>2</sub> or Ar. The following spectrometers were used: a 300 MHz GE-Omega (<sup>1</sup>H, <sup>31</sup>P NMR); a 500 MHz Bruker (<sup>1</sup>H NMR); a 490 MHz instrument (<sup>19</sup>F NMR); a MIDAC M1200 (FTIR); a HP-5971A MSD interfaced to a HP-5890 Series II GC (GC/MS). Elemental analysis was performed in Robertson Microlit Laboratories, Inc. (NJ).

**2-Amino-7,8-benzoquinoline.** Preparation was adapted from a known literature synthesis.<sup>9</sup> A suspension of 7,8-benzoquinoline and 4 equiv of NaNH<sub>2</sub> in *N,N*-dimethylaniline (DMA) was heated to 177 °C for 3 h under a continuous purge of dinitrogen. During this time the suspension underwent a color change from pale yellow, to dark green, and finally to dark brown. After cooling to room temperature, the mixture was hydrolyzed. The resulting organic layer was separated, dried over anhydrous MgSO<sub>4</sub>, filtered, and concentrated under vacuum to less than 1 mL. The amine was isolated from the mixture by flash chromatography over alumina, using hexanes to elute the DMA and unreacted benzoquinoline, followed by acetone to elute the ligand. After combining the fractions, solvent removal by rotoevaporation produced the compound as a pale orange solid (88% yield). <sup>1</sup>H NMR (CD<sub>2</sub>Cl<sub>2</sub>) δ in ppm: 9.07 (1H, m), 7.94 (1H, d, <sup>2</sup>J<sub>HH</sub> = 7.6), 7.83–7.87 (1H, m), 7.58–7.63 (4H, m), 6.83 (1H, d, <sup>2</sup>J<sub>HH</sub> = 8.6 Hz), 4.87 (NH<sub>2</sub>, s). Mp: 98–102 °C (lit.<sup>10</sup> 97–100 °C).

**2-Isopropylamino-7,8-benzoquinoline.** Synthesis of this ligand was analogous to the preparation of 2-amino-7,8-benzoquinoline: LiNH(*i*-Pr) was used instead of NaNH<sub>2</sub>, yielding the ligand as a bright yellow oil in 70% yield. <sup>1</sup>H NMR (CD<sub>2</sub>Cl<sub>2</sub>) δ in ppm: 1.36 (2 CH<sub>3</sub>, d, <sup>2</sup>J<sub>HH</sub> = 6.1 Hz), 4.39 (CH,

m), 4.72 (NH, d, <sup>2</sup>J<sub>HH</sub> = 7.6 Hz), 6.69 (1H, d, <sup>2</sup>J<sub>HH</sub> = 8.5 Hz), 7.50–7.62 (4H, m), 7.83–7.89 (2H, m), 9.10–9.13 (1H, m). Anal. Calcd for C<sub>16</sub>H<sub>16</sub>N<sub>2</sub>: C, 81.32; H, 6.82; N, 11.90. Found: C, 81.84; H, 6.61; N, 11.61.

**2-Methyl-7,8-benzoquinoline.** Synthesis of this ligand followed a known literature preparation method.<sup>12</sup> <sup>1</sup>H NMR (CD<sub>2</sub>Cl<sub>2</sub>) δ in ppm: 2.83 (CH<sub>3</sub>, s), 7.42 (1H, d, <sup>2</sup>J<sub>HH</sub> = 5.1 Hz), 7.67–7.89 (4H, m), 7.89–7.94 (1H, m), 8.08 (1H, d, <sup>2</sup>J<sub>HH</sub> = 5.2 Hz), 9.30–9.33 (1H, m). NMR data closely match literature values.<sup>12</sup>

**(2-Amino-7,8-benzoquinolinato)hydrido(aqua)bis-(triphenylphosphine)iridium(III) Tetrafluoroborate (3a).** [Ir(cod)(PPh<sub>3</sub>)<sub>2</sub>][BF<sub>4</sub>]<sup>21</sup> (200 mg, 0.242 mmol) and 2-amino-7,8-benzoquinoline (40 mg, 0.21 mmol) in CH<sub>2</sub>Cl<sub>2</sub> (10 mL) were treated with H<sub>2</sub> (1 atm, 20 mL/min) at 0° (ice bath) until the color of the solution changed from red to pale yellow (5 min). The volume of the solution was reduced by 50% in vacuo and hexanes–Et<sub>2</sub>O added (1:1 v/v, 10 mL) with stirring to precipitate a pale yellow solid (30 min), which was filtered, washed (hexanes, 5 mL), and dried in vacuo to give **3** (158 mg, 70% yield). <sup>1</sup>H NMR (298 K, CD<sub>2</sub>Cl<sub>2</sub>) δ in ppm: –16.43 (Ir–H, t, <sup>2</sup>J<sub>HP</sub> = 14.6 Hz); 1.92 (H<sub>2</sub>O, br s); 6.09 (NH<sub>2</sub>, br s); 6.5–8.8 (37 H, br m). <sup>31</sup>P{H} NMR (298 K, CD<sub>2</sub>Cl<sub>2</sub>) δ in ppm: 20.3 (s). Anal. Calcd for C<sub>39</sub>H<sub>42</sub>N<sub>2</sub>OP<sub>2</sub>BF<sub>4</sub>Ir: C, 55.93; H, 4.14; N, 2.76. Found: C, 55.82; H, 4.17; N, 3.03.

**(2-Isopropylamino-7,8-benzoquinolinato)hydrido(aqua)bis-(triphenylphosphine)iridium(III) Tetrafluoroborate or Hexafluorophosphate (3b).** Preparation of **3b** was analogous to the synthesis of **3a**, substituting 2-isopropylamino-7,8-benzoquinoline for 2-amino-7,8-benzoquinoline. **3b** was obtained in 78% yield. <sup>1</sup>H NMR (CD<sub>2</sub>Cl<sub>2</sub>) δ in ppm: –16.10 (Ir–H, t, <sup>2</sup>J<sub>HP</sub> = 14.4 Hz); 1.30 (CH(CH<sub>3</sub>)<sub>2</sub>, d, <sup>2</sup>J<sub>HH</sub> = 5.9 Hz); 3.93 (–CH(CH<sub>3</sub>)<sub>2</sub>, m); 6.16 (NH, br s), 6.6–7.8 (37H, m). <sup>31</sup>P{H} NMR (CD<sub>2</sub>Cl<sub>2</sub>) δ in ppm: 20.42 (s). Anal. Calcd for C<sub>52</sub>H<sub>48</sub>N<sub>2</sub>OP<sub>2</sub>PF<sub>6</sub>Ir: C, 56.0; H, 4.33; N, 2.51. Found: C, 55.91; H, 4.76; N, 2.70.

**(2-Methyl-7,8-benzoquinolinato)hydrido(aqua)bis-(triphenylphosphine)iridium(III) Tetrafluoroborate (3c).** Preparation of **3c** was analogous to the synthesis of **3a**, substituting 2-methyl-7,8-benzoquinoline for 2-amino-7,8-benzoquinoline. **3c** was obtained in 80% yield. <sup>1</sup>H NMR (CD<sub>2</sub>Cl<sub>2</sub>) δ in ppm: –14.06 (Ir–H, br s); 2.35 (CH<sub>3</sub>, s); 6.7–8.0 (37H, m). <sup>31</sup>P{H} NMR (CD<sub>2</sub>Cl<sub>2</sub>) δ in ppm: 22.97 (s). Anal. Calcd for C<sub>50</sub>H<sub>43</sub>IrNOP<sub>2</sub>BF<sub>4</sub>: C, 59.20; H, 4.27; N, 1.38. Found: C, 58.88; H, 4.44; N, 1.20.

**(2-Amino-7,8-benzoquinolinato)hydrido(fluoro)bis-(triphenylphosphine)iridium(III) (4a).** To complex **3a** (250 mg, 0.25 mmol) in stirred acetone (10 mL) was added [*n*-Bu<sub>4</sub>N]F (0.25 mL of 1 M thf solution, 0.25 mmol). After 10 min, hexanes (10 mL) were added to give a pale yellow solid, which was filtered, washed (hexanes, 10 mL), and dried in vacuo (230 mg). Recrystallization from CH<sub>2</sub>Cl<sub>2</sub>–hexanes gave **4a** (163 mg, 65% yield). <sup>1</sup>H NMR (298 K, CD<sub>2</sub>Cl<sub>2</sub>) δ in ppm: –16.13 (Ir–H, td, <sup>2</sup>J<sub>HP</sub> = 17 Hz, <sup>2</sup>J<sub>HF</sub> = 4.8 Hz); 6.03 (1H, <sup>2</sup>J<sub>HH</sub> = 9 Hz); 6.42 (1H, t, <sup>2</sup>J<sub>HH</sub> = 7.2 Hz); 6.67 (1H, d, <sup>2</sup>J<sub>HH</sub> = 6.6 Hz); 6.9–8.5 (36H, m). <sup>1</sup>H NMR (193 K, CD<sub>2</sub>Cl<sub>2</sub>) δ in ppm: 10.05 (N–H···F, d, <sup>1</sup>J<sub>HF</sub> = 52 Hz); 4.85 (N–H, br s). <sup>31</sup>P{H} NMR (183 K, CD<sub>2</sub>Cl<sub>2</sub>) δ in ppm: 16.4 (d, <sup>2</sup>J<sub>PF</sub> = 21 Hz). <sup>19</sup>F NMR (298 K, CD<sub>2</sub>Cl<sub>2</sub>, with CFCl<sub>3</sub> ref) δ in ppm: –328 (t, <sup>2</sup>J<sub>PF</sub> = 21 Hz); (193 K CD<sub>2</sub>Cl<sub>2</sub>) –323 (br s). Anal. Calcd for C<sub>49</sub>FH<sub>40</sub>IrN<sub>2</sub>P<sub>2</sub>: C, 63.29; H, 4.31; N, 3.01. Found: C, 63.11; H, 4.17; N, 3.05.

**(2-Isopropylamino-7,8-benzoquinolinato)hydrido(fluoro)bis-(triphenylphosphine)iridium(III) (4b).** With **3b** as the starting material, the synthesis of **4b** was analogous to the preparation of **4a**. **4b** was obtained in 70% yield after recrystallization. <sup>1</sup>H NMR (CD<sub>2</sub>Cl<sub>2</sub>) δ in ppm: –16.09 (Ir–H, td, <sup>2</sup>J<sub>HP</sub> = 16.7 Hz, <sup>2</sup>J<sub>HF</sub> = 5.6 Hz); 0.96 (CH(CH<sub>3</sub>)<sub>2</sub>, d, <sup>2</sup>J<sub>HH</sub> = 6.6 Hz); 3.33 (CH(CH<sub>3</sub>)<sub>2</sub>, m); 6.13 (1H, d, <sup>2</sup>J<sub>HH</sub> = 8.7 Hz); 6.36

(19) Kulawiec, R. J.; Crabtree, H. C. *Coord. Chem. Rev.* **1990**, *99*, 89.

(20) Lee, D.-H.; Patel, B. P.; Clot, E.; Eisenstein, O.; Crabtree, R. H. *J. Chem. Soc., Chem. Commun.* **1999**, 297.

(21) Haines, L. M.; Singleton, E. *J. Chem. Soc., Dalton Trans.* **1972**, 1891.



(1H, t,  $^2J_{\text{HH}} = 6.0$  Hz); 6.57 (1H, d,  $^2J_{\text{HH}} = 6.9$  Hz); 6.8–7.5 (34H, m); 10.26 (N–H···F, d,  $^1J_{\text{HF}} = 49.6$  Hz).  $^{31}\text{P}\{^1\text{H}\}$  NMR ( $\text{CD}_2\text{Cl}_2$ )  $\delta$  in ppm: 14.89 (d,  $^2J_{\text{PF}} = 21.5$  Hz). Anal. Calcd for  $\text{C}_{52}\text{FH}_{46}\text{IrN}_2\text{P}_2$ : C, 64.20, H, 4.77; N, 2.88. Found: C, 64.55; H, 4.32; N, 2.49.

**(2-Methyl-7,8-benzoquinolino)hydrido(fluoro)bis(triphenylphosphine)iridium(III) (4c).** With **3c** as the starting material, the synthesis of **4c** was analogous to the preparation of **4a**. **4c** was obtained in 73% yield.  $^1\text{H}$  NMR ( $\text{CD}_2\text{Cl}_2$ )  $\delta$  in ppm: –17.5 (Ir–H, td,  $^2J_{\text{HP}} = 15$  Hz,  $^2J_{\text{HF}} = 4.7$  Hz); 2.12 ( $\text{CH}_3$ , s); 6.49 (1H, t,  $^2J_{\text{HH}} = 7.0$  Hz); 6.8–7.4 (35H, m); 7.59 (1H, d,  $^2J_{\text{HH}} = 8.5$  Hz).  $^{31}\text{P}\{^1\text{H}\}$  NMR ( $\text{CD}_2\text{Cl}_2$ )  $\delta$  in ppm: 12.46 (d,  $^2J_{\text{PF}} = 22$  Hz). Anal. Calcd for  $\text{C}_{50}\text{FH}_{41}\text{IrNP}_2$ : C, 64.60, H, 4.45; N, 1.51. Found: C, 64.73; H, 4.53; N, 1.43.

**Observation of HF Complex 6a.** To complex **4a** (5 mg, 5.4  $\mu\text{mol}$ ) in  $\text{CD}_2\text{Cl}_2$  (0.5 mL) in an NMR tube at 195 K (acetone–dry ice) was added  $\text{HBF}_4\cdot\text{Et}_2\text{O}$  (1  $\mu\text{L}$ , 5.8  $\mu\text{mol}$ ). After rapid transfer to a precooled NMR probe, NMR data were obtained.  $^1\text{H}$  NMR (183 K,  $\text{CD}_2\text{Cl}_2$ )  $\delta$  in ppm: –16.31 (Ir–H, br s); 6.64 (1H, t); 6.84 (NH<sub>2</sub>, br s); 6.99–8.25 (36H, m); 9.77 (Ir–F–H, d,  $^1J_{\text{HF}} = 440 \pm 5$  Hz).  $^{19}\text{F}$  NMR (183 K,  $\text{CD}_2\text{Cl}_2$ )  $\delta$  in ppm: –178 (Ir–F–H, d,  $440 \pm 5$  Hz).  $^{31}\text{P}\{^1\text{H}\}$  NMR (183 K,  $\text{CD}_2\text{Cl}_2$ )  $\delta$  in ppm: 21.54 (d,  $^2J_{\text{PF}} = 12$  Hz). The compound decomposes above 210 K; therefore no isolation or elemental analysis was possible.

**Observation of HF Complex 6b.** To complex **4b** (5.5 mg, 5.7  $\mu\text{mol}$ ) in  $\text{CD}_2\text{Cl}_2$  (0.5 mL) in an NMR tube at 195 K (acetone–dry ice) was added  $\text{HBF}_4\cdot\text{Et}_2\text{O}$  (1  $\mu\text{L}$ , 5.8  $\mu\text{mol}$ ). After rapid transfer to a precooled NMR probe, NMR data were obtained.  $^1\text{H}$  NMR (183 K,  $\text{CD}_2\text{Cl}_2$ )  $\delta$  in ppm: –16.25 (Ir–H, br s); 1.16 (–CH( $\text{CH}_3$ )<sub>2</sub>, d,  $^2J_{\text{HH}} = 63.8$  Hz), 3.91 (CH( $\text{CH}_3$ )<sub>2</sub>, s), 6.5–7.5 (38H, m), 9.89 (Ir–F–H, d,  $^1J_{\text{HF}} = 430 \pm 5$  Hz). No isolation or elemental analysis was possible due to decomposition of the product.

**X-ray Structural Analysis of Complex 3b·CF<sub>3</sub>SO<sub>3</sub>·CH<sub>2</sub>Cl<sub>2</sub> and 4a.** Suitable crystals for single-crystal X-ray diffraction (0.30 × 0.15 × 0.01 mm, **3b**·CF<sub>3</sub>SO<sub>3</sub>·CH<sub>2</sub>Cl<sub>2</sub>; 0.30 × 0.20 × 0.20 mm, **4a**) were selected and mounted on the tip of a

capillary with epoxy cement. The data were collected on a Siemens P4 diffractometer equipped with a SMART/CCD detector.

The structures were solved by direct methods, completed by subsequent difference Fourier syntheses, and refined by full-matrix, least-squares procedures. An empirical absorption correction (DIFABS) was applied to the data of **3b**·CF<sub>3</sub>SO<sub>3</sub>·CH<sub>2</sub>Cl<sub>2</sub>, based on a Fourier series in the polar angles of the incident and diffracted beam paths, and was used to model an absorption surface for the difference between the observed and calculated structure factors. No corrections were required for **4a** because there was less than 10% variation in the integrated  $\psi$ -scan intensities. The carbons C(5), C(24), C(44), and C(56) of **3b**·CF<sub>3</sub>SO<sub>3</sub>·CH<sub>2</sub>Cl<sub>2</sub> were persistently nonpositive definite and were refined isotropically. All other non-hydrogen atoms were refined with anisotropic displacement parameters. The hydride hydrogen atoms and the hydrogen atoms on the aqua ligand of **3b**·CF<sub>3</sub>SO<sub>3</sub>·CH<sub>2</sub>Cl<sub>2</sub> could not be located and were ignored in the refinement, but not in the calculation of the intensive properties of the crystal. The hydride hydrogen atom of **4a** was located from the difference map and allowed to refine. All other hydrogen atoms were treated as idealized contributions. Several peaks from the final difference map of **3b**·CF<sub>3</sub>SO<sub>3</sub>·CH<sub>2</sub>Cl<sub>2</sub> (1.3–2.3 e/Å<sup>3</sup>) remained, but were in chemically unreasonable positions (0.9–1.5 Å from iridium) and were considered noise.

**Acknowledgment.** We thank the NSF for support.

**Supporting Information Available:** Tables of atomic coordinates, bond distances, bond angles, anisotropic displacement coefficients, and hydrogen atom coordinates for the structural analyses of compounds **3b**·CF<sub>3</sub>SO<sub>3</sub>·CH<sub>2</sub>Cl<sub>2</sub> and **4a**. This material is available free of charge via the Internet at <http://pubs.acs.org>.

OM9809769